Received: 14 August 2020 | Revised: 16 October 2020 | Accepted: 16 October 2020

DOI: 10.1111/jace.17541

Journal of the American Ceramic Society

ORIGINAL ARTICLE

Influence of pressure and dwell time on pressure-assisted sintering of calcium cobaltite

Sophie Bresch[1] | **Björn Mieller**[1] | **Daniela Schönauer-Kamin**[2] | **Ralf Moos**[2] | **Timmy Reimann**[3] | **Fabien Giovannelli**[4] | **Torsten Rabe**[1]

[1]Division Advanced Technical Ceramics, Bundesanstalt für Materialforschung und –prüfung (BAM), Berlin, Germany

[2]Department of Functional Materials, University of Bayreuth, Bayreuth, Germany

[3]INNOVENT e.V. Technologieentwicklung, Jena, Germany

[4]Université de Tours, CNRS, INSA, GREMAN UMR 7347, IUT de Blois, Blois Cedex, France

Correspondence
Sophie Bresch, Division Advanced Technical Ceramics, Bundesanstalt für Materialforschung und –prüfung (BAM), 12203 Berlin, Germany.
Email: Sophie.Bresch@bam.de

Abstract

Calcium cobaltite $Ca_3Co_4O_9$, abbreviated Co349, is a promising thermoelectric material for high-temperature applications in air. Its anisotropic properties can be assigned to polycrystalline parts by texturing. Tape casting and pressure-assisted sintering (PAS) are a possible future way for a cost-effective mass-production of thermoelectric generators. This study examines the influence of pressure and dwell time during PAS at 900°C of tape-cast Co349 on texture and thermoelectric properties. Tape casting aligns lentoid Co349. PAS results in a textured Co349 microstructure with the thermoelectrically favorable ab-direction perpendicular to the pressing direction. By pressure variation during sintering, the microstructure of Co349 can be tailored either toward a maximum figure of merit as required for energy harvesting or toward a maximum power factor as required for energy harvesting. Moderate pressure of 2.5 MPa results in 25% porosity and a textured microstructure with a figure of merit of 0.13 at 700°C, two times higher than the dry-pressed, pressureless-sintered reference. A pressure of 7.5 MPa leads to 94% density and a high power factor of 326 μW/mK^2 at 800°C, which is 11 times higher than the dry-pressed reference (30 MPa) from the same powder.

KEYWORDS

hot pressing, texture, thermoelectric properties

1 | INTRODUCTION

The direct conversion of heat into electricity by thermoelectric generators is a promising approach to generate power for sensor systems in hot and harsh environments. For this special application, thermoelectric oxides are especially interesting, as they can be used at high temperatures up to 800°C in air. Thermoelectric materials in general are evaluated by the power factor $PF = S^2 \bullet \sigma$ and the figure of merit $ZT = (PF \bullet T)/\kappa$. For infinite heat sources as in the field of energy harvesting, the thermoelectric material should be optimized for maximum PF to enable a high-power generation.[1] For a limited heat source as in the field of energy recovery, a high-energy conversion efficiency is required and thus a maximum ZT is important.[1] Thermoelectric oxides, although having lower ZT than conventional thermoelectric materials like tellurides and skutterudites,[2] are an interesting alternative at elevated temperatures as they are stable in air. In

addition, their raw materials are less toxic and more abundant.[2,3] One of the most promising oxide p-type materials is calcium cobaltite $Ca_3Co_4O_9$ (in the following abbreviated by Co349).[2-7] It has a layered misfit crystal structure of alternating layers of a hexagonal CoO_2 sublattice and a triple rocksalt type Ca_2CoO_3 sublattice.[4,8] Co349 has a plate-like, lentoid grain morphology due to an increased grain growth in ab-direction.[3] Due to its crystal structure, the physical and thermoelectric properties of single-crystal Co349 are strongly anisotropic.[9,10] The electrical conductivity of single-crystal whiskers is 500 to 1000 times higher in ab-direction than in c-direction ($\sigma_{ab} = 500\ldots1000 \bullet \sigma_c$).[3] Hot-pressed samples with 10 MPa show anisotropic Seebeck coefficients $S_{ab} = 1.06 \bullet S_c$ and anisotropic thermal conductivity $\kappa_{ab} = 2.04 \bullet \kappa_c$.[10] Co349 decomposes at 926°C. This limits the sintering temperature and thereby the densification in the case of conventional sintering.[3,11]

The anisotropy of the particle can be assigned to the polycrystalline material by texturing the microstructure. A detailed literature review about the texturing of Co349 can be found in our previous work[12] or by Prasad et al.[13] Here we only focus on some aspects of texturing Co349. Dry-pressing with high pressure up to 1000 MPa is a simple way to increase texture,[7,14] but the sample size is limited. Casting a slurry composed of anisotropic particles and organic binders by the doctor-blade method into a tape is a well-known technique to texture materials.[15-17] The effect can be enforced by implementing a fraction of large anisotropic grains (>10 μm), known as templated grain growth.[18] The tape-cast specimens by Schulz et al[16] showed anisotropic microstructure and high porosity (45%). Due to the latter, electrical conductivity and *PF* were not improved compared with the dry-pressed reference (300 MPa). Nagahamo et al[18] doubled the electrical conductivity using templated grain growth and tape casting (600 S/m at 400°C) compared to a nontextured compound fabricated by cold isostatic pressing. Applied pressure during sintering increases both sinter density and texture. Several groups applied hot-pressing (or sinter-forging, respectively) with pressures from 5 MPa to 50 MPa.[5,10,19] The Co349 specimens were highly textured and nearly fully dense. With a pressure of 30 MPa, Kenfaui et al[9] reached $\sigma(900K) = 8 \bullet \sigma_{ref}$. Due to the enhanced charge carrier mobility in ab-direction, the thermal conductivities of hot-pressed specimens measured in ab-direction are enhanced by the factor of 10[12] or 4.7[10] compared to the reference. Liu et al[20] and Delorme et al[21] used spark plasma sintering (SPS) with a pressure of 50 MPa[20] (70 MPa[21]). A relative density of > 98% was reached with $\sigma = 12\,000$ S/m $= 3.5 \bullet \sigma_{ref}$. Comparing SPS and hot-pressing, the latter leads to a higher anisotropy and higher *PF*.[22] Finally, a combination of texturing during shaping at room temperature and texturing during sintering is possible. Schulz et al[16] combined tape casting and pressure-assisted sintering. Pressure-assisted sintering is a sintering technology known from the field of low-temperature co-fired ceramics (LTCC) using a moderate uniaxial pressure during sintering and a different pressing plate setup than hot-pressing.[23] Pressures of 7.5 MPa and 10 MPa during sintering led to nearly fully dense specimens with very high electrical conductivities in ab-direction ($\sigma(1000\ K) = 17\,000$ S/m[16]).

Tape casting has much potential for texturing Co349 as shown by Schulz et al.[16] It is widely used in the field of electroceramics,[15] for example, for LTCC,[15,24] piezo actuators,[24,25] or lambda-probes,[26] and it can be used to design thermoelectric generators (TEG).[16,27-29] It is easily scalable and an approach for inexpensive mass production of TEG-stacks. Due to the low density of conventionally sintered Co349, the produced parts are fragile. Based on the work of Schulz et al,[16] we recently reported on the combination of tape casting and pressure-assisted sintering to texture Co349.[12] In this work,[12] we focused on the influence of powder composition on the thermoelectric properties when using pressure-assisted sintering. We found that Bi-doping ($Ca_{2.7}Bi_{0.3}Co_4O_9$) is not beneficial as it leads to distortions and abnormal grain growth due to a liquid phase when a pressure of 10 MPa is applied during sintering. The microstructure of the samples from undoped Co349 fabricated with pressure-assisted sintering showed strong texture, high sinter density, and thus both electrical conductivity and *PF* in ab-direction were strongly increased by more than a factor of 10 compared to the dry-pressed sample from the same powder. Due to the high density (94%), κ_{ab} increased as well for the PAS-samples, which nearly compensated the benefits of texturing regarding ZT_{ab}. It would be favorable to apply a moderate pressure during PAS to benefit from texturing on the one hand and to maintain a certain porosity to decrease κ_{ab}. Hence, in this work we focus on the influence of pressure and dwell time during PAS on the thermoelectric properties of undoped Co349 to optimize either *PF* or *ZT*.

2 | EXPERIMENTAL PROCEDURE

$Ca_3Co_4O_9$ was synthesized by solid-state reaction. Stochiometric amounts of the raw material Co_3O_4 (99.97+ %, ChemPUR, Karlsruhe, Germany) and $CaCO_3$ (99%, low-alkali, Riedel-de Haën, Seelze, Germany) were attrition-milled (moliNEx, Netzsch, Selb, Germany) for 45 minutes at 800 rpm using ZrO_2 grinding media ($d = 2.5$ mm). The powder mixture was calcined at 900°C for 12 hours in air to obtain $Ca_3Co_4O_9$. The calcined powder was grinded in a planetary ball mill (Pulverisette 5, Fritsch, Idar-Oberstein, Germany) for 20 minutes with agate grinding balls and subsequently attrition-milled for 15 minutes to obtain $Ca_3Co_4O_9$ powder with a $d_{50} = 3$ μm (particle size distribution determined with laser diffraction system, Mastersizer 2000, Malvern Instruments, Malvern, United

Kingdom) and a specific surface of 3 m^2/g (BET, NOVA 2200, 3P INSTRUMENTS, Odelzhausen, Germany). This powder was mixed with polyvinyl butyral (Eastman, Kingsport, US), dibutylphtalate (ACROS organics, Fair Lawn, US), rhodafac RE-610 (Solvay, Hannover, Germany), ethanol (Merck, Darmstadt, Germany), methylethylketone (Merck, Darmstadt, Germany) and cyclohexanone (Merck, Darmstadt, Germany) in a porcelain mill for one day to obtain a tape-casting slurry. The slurry was tape-cast with doctor-blades on a tape-casting machine (Netsch, Selb, Germany) to produce a ceramic green tape with a mean thickness of 70 μm and an organic content of 12 wt% (loss on ignition at 450°C). The tape was cut into 70 mm × 70 mm sheets using a special manual punching tool. The sheets were laminated with 20 MPa at 70°C in a uniaxial press using a custom-made heated stacking tool. To prevent reactions with the pressing plates, commercial Al_2O_3-tape (Ceratape A, CeramTec, Plochingen, Germany) was laminated on the top and on the bottom of the samples. The laminates were sintered at 900°C in a commercial LTCC-sinter press (PEO-630, ATV Technologie GmbH, Vaterstetten, Germany). The process chain is illustrated in Figure 1. The pressure during sintering was varied between 0 MPa and 7.5 MPa and the dwell time was varied between 2 hours and 8 hours, respectively. After sintering, the alumina tape and a small reaction layer (2 μm) were removed by scrubbing, and samples were cut in the desired geometries for the different measurements using different precision cut-off machines. Reference samples were prepared by dry-pressing of the same powder (+ 1.5 wt% pressing additives) with 30 MPa into discs with a diameter of 25 mm and bars with a length of 50 mm and sintered at 900°C for 24 hours in air without pressure. After sintering, the specimens were cut in the desired geometries. The detailed experimental setup is shown in Table 1.

Phase content of the starting powder as well as of the sintered reference and the sintered laminates were analyzed using X-ray diffraction (XRD) with Co-Kα radiation (XRD 3000 PTS, Seifert, Schnaittach-Hormersdorf, Germany). The anisotropy was characterized by measuring pole figures of (002) and (111) lattice planes (Phi $\phi = 0$ - 360°, Psi $\chi = 0$-70°, increment $\Delta\chi = 5°$) using XRD with Co-*Kα* radiation (D8 Discover, Bruker, Billerica, US). In order to get a proper measuring point distribution of the pole figures, the increment $\Delta\phi$ was defined by the following equation: $\cos(\Delta\phi(\chi)) \approx (\cos(\Delta\chi) - \sin^2\chi)/\sin^2\chi$. Bruker DIFFRAC Texture software was used to export the pole figure data. Background correction, plotting and further evaluation was performed with MTEX toolbox 5.2.8[30] for MATLAB (The MathWorks Inc, Natick, US).

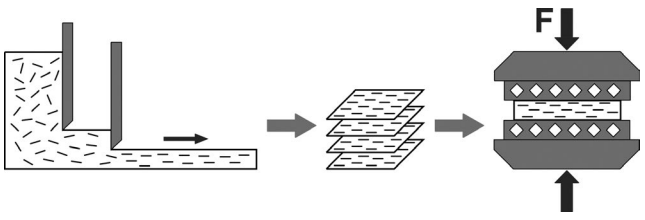

FIGURE 1 Scheme of the simplified manufacturing process of the PAS laminates. Small black rectangles illustrate the orientation of Co349 particles. Not to scale

The morphology of the powder as well as the microstructure of the different specimens were examined with scanning electron microscopy (Gemini Supra 40, ZEISS, Jena, Germany). To examine the grain size of the sintered specimens (thermally etched surface [900°C for 30 minutes], with SE detector), the maximum Feret diameters of at least 100 grains were measured using the imaging software ImageJ. Archimedes method was used to measure the bulk density ρ of the sintered samples according to $\rho = (\rho_w \bullet m_1)/(m_3 - m_2)$ with the density of water ρ_w, the dry mass of the sample m_1, the apparent mass of the sample under water m_2 and the soaked with water mass of the sample m_3. The true density ρ_{true} of the powder was determined with a He-Pycnometer (AccuPyc II 1340, Micromeritics) and used to calculate the relative density $\rho_{rel} = (100\% \bullet \rho)/(\rho_{true})$. The Seebeck coefficient at room temperature was measured with a laboratory setup using type K thermocouples as measuring tips and Peltier elements for heating and cooling. The measuring procedure and its validation are explained in detail in reference 31. The same setup was used to determine the electrical conductivity σ of the samples according to $\sigma = (R \bullet h \bullet w)/l$. The dimensions ($h$, w, l) between the measurement tips were measured with an optical microscope and the resistance R of the samples with a 4-wire setup using a digital multimeter (8808A, Fluke). The thermal conductivity κ of the reference sample was calculated according to $\kappa = a \bullet c_p \bullet \rho$. The thermal diffusivity a was measured by laser flash method (LFA 457, Netzsch, Selb, Germany) from room temperature up to 1000 K in air. The heat capacity c_p of the material was measured by differential scanning calorimetry (STA449F3 Jupiter, Netzsch, Selb, Germany) in N_2 with a heating rate of 20 K/min up to 1000 K. The thermal conductivity of the textured samples in ab-direction κ_{ab} was measured with hot-disc method with a slab module (Hot Disk TPS 2500S, C3 Prozess- und Analysetechnik GmbH, Haar, Germany) at room temperature. For the detailed measurement setup, the reader is referred to reference 12.

To derive the Seebeck coefficients and the electrical conductivities at elevated temperatures, the bar-like samples were contacted by two Au/Pt-thermocouples and by four platinum electrodes. The electrical conductivity was measured in four-wire technique via the platinum contacts. To determine the Seebeck coefficients, the temperature difference ΔT over the specimens was measured by the Au/Pt-thermocouples

TABLE 1 Influence of pressure and dwell time during sintering on material properties

p in MPa	*t* in h	rel. Density in %	MRD	*S* in μVK^{-1}	σ in Scm^{-1}	*PF* in $\mu Wm^{-1}K^{-2}$	κ in $Wm^{-1}K^{-1}$	*ZT* in 10^{-3}
0 (ref)	2	49.9 ± 0.2	3.5 [9]	120.2 ± 0.2	9 ± 1	14 ± 6	0.40 ± 0.01	12 ± 2
0	2	57.2 ± 0.1	9.2	124.0 ± 0.5	29 ± 5	44 ± 1		
2.5	2	74.8 ± 4.4	12.1	124.6 ± 0.3	94 ± 31	146 ± 48	1.70 ± 0.01	26 ± 9
2.5	4	78.3 ± 1.3		123.9 ± 0.3	96 ± 14	148 ± 21		
2.5	8	80.7 ± 0.3		124.5 ± 0.4	126 ± 28	195 ± 43		
5.0	2	84.3 ± 1.5		126.1 ± 0.5	128 ± 29	203 ± 45		
7.5	2	93.5 ± 0.8	12.8	135.4 ± 6.1	151 ± 11	279 ± 43	4.03 ± 0.02	21 ± 3
7.5	8	94.7 ± 0.3	12.8	146.9 ± 0.5	140 ± 2	302 ± 6		

Note: Relative density, *S*, σ, and κ (all at room temperature) are given with standard deviation. For *PF* and *ZT*, the error according to Gaussian error propagation is given. MRD of dry-pressed test bar is derived from reference [9].

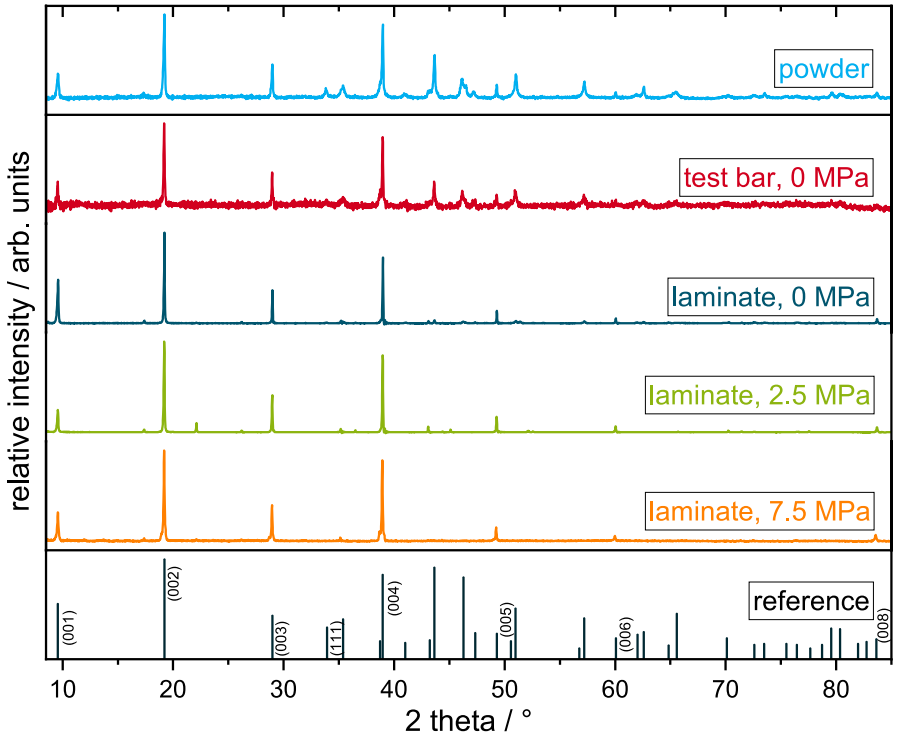

FIGURE 2 XRD pattern (λ = Co-$K\alpha$) of Co349 powder, sintered test bars and sintered laminates with different pressure and 2 h dwell time; reference values for $Ca_3Co_4O_9$ taken from [8]

and the thermoelectric voltage ΔU was measured in-between the platinum contacts of the thermocouple. A modulated temperature gradient ΔT of around 20 K over the bar-like specimens was applied by an additional heater. The contacted samples were mounted in a special sample holder placed in gas-flushable tube furnace, which was purged by dry synthetic air. The measurements were performed stepwise from 900°C to room temperature. The Seebeck coefficient *S* was calculated as described in reference 32. The measurement setup is indirectly validated with another Seebeck measurement system.

Minitab 17 was used to statistically analyze the data. The data samples were tested for differences in mean value with two-sample t-test and for differences in standard deviation with F-test with a level of significance set to 5%. The sample size (number) of the room temperature data was at least 5, and of the high-temperature data at least 3.

3 | RESULTS AND DISCUSSION

3.1 | Phase content, microstructure, and texture

The XRD patterns of the starting Co349 powder, the sintered test bars, and the sintered laminates as well as a reference pattern[8] are shown in Figure 2. Comparing the starting powder with the reference, no detectable impurities are visible, which indicates a successful calcination process. The pressureless-sintered test bar has a similar

pattern as the calcined powder, the intensity ratio between (111) and (004) reflection is 0.16 smaller than the value of the powder (0.37). This indicates a weak texturing due to dry-pressing. The (001) reflections of the tape cast and pressureless-sintered laminates are strongly increased, supporting the assumption of a texturation during tape casting. The PAS laminates show only (001) peaks, indicating a very strong texture. The laminate sintered with 2.5 MPa shows an additional peak at 22°. This could be the (111) peak of Co_3O_4. Co_3O_4 is formed as a reaction layer between the release tape (Al_2O_3) and Co349. Usually, the reaction layer was removed after sintering. The peak indicates an incomplete removal of the reaction layer.

Figure 3 illustrates the microstructure of the different specimens. The calcined powder (see Figure 3A) has the typical flake-like morphology of Co349.[3] Due to the milling, the single-crystal layers are visible. As shown in Figure 3B, the grains are rounded after sintering at 900°C without pressure (reference sample – not tape-cast). Sinter necks are visible, but the structure is still very porous. Sintering without pressure is not sufficient to obtain a dense microstrucutre at 900°C. The sinter necks and pores indicate that the thermal treatment only leads to a first stage sintering.[33] After tape casting, a slight particle orientation is visible in the SEM images (see Figure 3C). The pressureless-sintered laminate shown in Figure 3D) has a slightly different microstructure than the sintered test bar. The grains are smaller and the microstructure is still very porous. Considering the results from the XRD measurements (see Figure 2), tape casting leads already to a textured microstructure. As illustrated in Figure 3E) the fracture surface of a laminate sintered with a uniaxial pressure of 5 MPa for 2 hours is very dense without large pores. The laminar crystal structure is visible. It is difficult to detect single grains at a fracture surface or a polished surface. Therefore, the polished surfaces of the PAS specimens were thermally etched at 900°C for 30 min (Figure 3F-H). Etching reveals that the microstructure includes pores. The grains are between 1 and 3 μm long and about 1 μm thick. All thermally etched specimens show fine white particles ($l \approx 160$ nm, $h \approx 80$ nm). EDX-point analysis (8kV, 150 000×) of nearly free-standing white particles revealed that they are Co-enriched (Co-L: 41 at% versus 29 at% for the matrix) and Ca-deficient (Ca-K: 5 at% versus 16 at% for the matrix). We, therefore, suppose that these are Co_3O_4-nanoparticles, probably an effect of polishing and thermal etching as these particles are not found in the fractured samples. As shown in Figure 3F-H), the number of pores decreases with increasing pressure. At 7.5 MPa the microstructure appears to be completely dense (see Figure 3H). An increased dwell time does not seem to increase the densification remarkably (Figure 3F,I). Comparing Figure 3F) with Figure 3I), longer dwell times increase the grain size from 1.5 ± 0.7 μm to 2.4 ± 0.8 μm. It can be concluded that pressure-assisted sintering is a good way to obtain a dense textured microstructure of Co349. Pressure during sintering works as an additional driving force and therefore is an effective way to support densification. Higher pressure apparently leads to improved densification. Longer dwell times increase the grain size but not the densification.

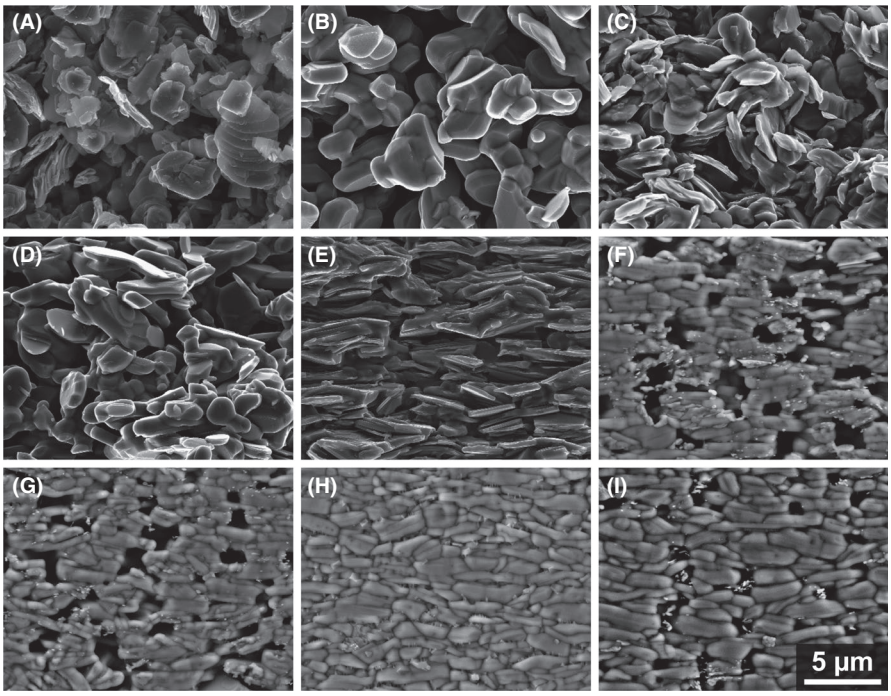

FIGURE 3 Micrographs of (A-E) fracture surfaces with InLense detector showing: (A) Co349 powder; (B) sintered test bar—0 MPa, 24 h; (C) green laminate; (D) sintered laminate—0 MPa, 2 h; (E) PAS laminate—5 MPa, 2 h. Micrograph of (F-I) thermally etched polished surfaces with SE-detector showing (F) PAS laminate—2.5 MPa, 2 h; (G) PAS laminate—5 MPa, 2 h; (H) PAS laminate—7.5 MPa, 2 h; and (I) PAS—laminate—2.5 MPa, 8 h

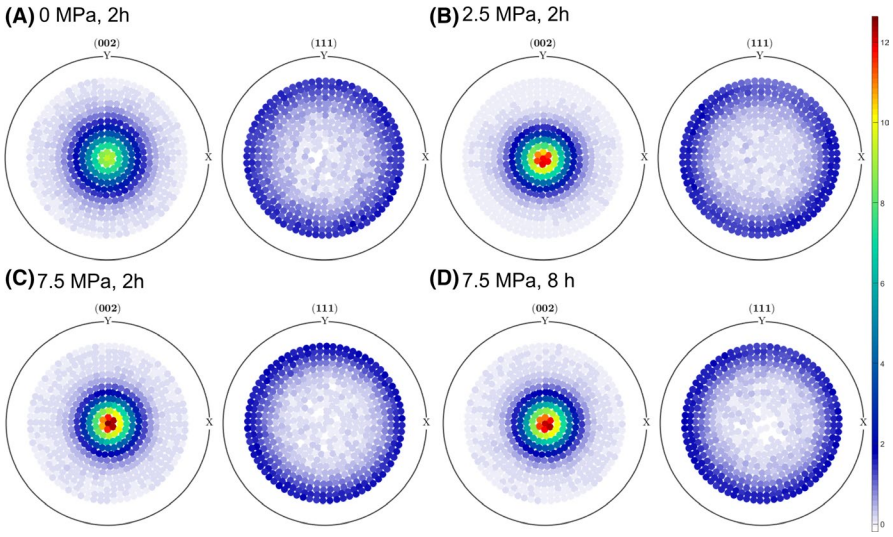

FIGURE 4 XRD pole figures (002) and (111) with intensity scale in a.u. of Co349 samples: (A) sintered laminate with 0 MPa, 2 h; (B-D) PAS laminate with varying pressures and dwell times

To determine the influence of the pressure during sintering on texture, the latter was analyzed using XRD pole figures of (002) and (111) reflections as shown in Figure 4. All tape cast samples show a strong fiber texture with a preferential orientation of the c-axis orthogonal to the tape casting direction. Multiples of a random distribution (MRD) in out of plane direction were calculated from estimated orientation density function (ODF) data (MTEX Software) to quantify the texturing (see Table 1). The MRD can vary from 1 (no texture) to infinty (single crystal). As the texture of the dry-pressed bar was not measured, in Figure 5A) the MRD data of a similar processed Co349 test bar were used as a reference [9]. The reference exhibits a low degree of texture. The tape cast sample prior to sintering already shows a strong fiber texture (MRD = 9.3). Sintering without pressure does not increase the texture effect (Figure 4A). PAS increases the texturing with the c-axis parallel to the pressing direction (see Figure 4B-D and Figure 5A). With increasing pressure, the texture gets stronger (Figure 4C) and reaches a maximum MRD of 12.8. Longer dwell times do not increase the texturing as shown in Figure 4D).

3.2 | Density

The relative density (after sintering) of the dry-pressed samples is with 50% very low (Table 1) in comparison with other

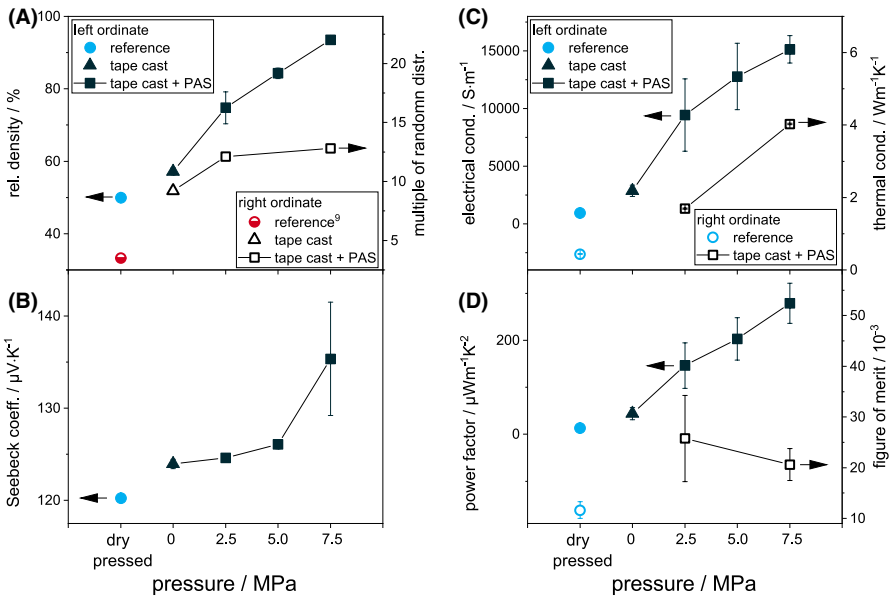

FIGURE 5 Physical and thermoelectric properties at room temperature of test bar and laminate: (A) relative sinter density and multiples of randomn distibution; (B) Seebeck coefficient; (C) electrical and thermal conductivity; and (D) power factor and figure of merit. The multiples of a random distribution (MRD) of a dry-pressed test bar is derived from reference [9]. The laminates were sintered with different pressures for a dwell time of 2 h. Error bars of *ZT* and *PF* indicate calculated errors according to Gaussian error propagation, the other error bars indicate the standard deviation

studies.[9,16,34] But in these studies, higher pressures during dry-pressing (up to 300 MPa) were applied, resulting in higher green-densities and thus higher sinter-densities (60% to 72%). Tape casting increases the relative density to 57%, but the parts are still very fragile when no pressure is applied during sintering. Increased density due to tape casting is described in literature.[15] With increasing uniaxial pressure, the relative density increases to 94% for 7.5 MPa (Figure 5A). The increase in the relative density as a function of pressure during sintering fits a linear regression within this experimental framework. The relative density of the PAS specimens is in the range of the hot-pressed samples observed by Kenfaui et al.[9]

3.3 | Seebeck coefficient

The Seebeck coefficient at room temperature S(22°C) increases by 3% when tape casting is used (Figure 5B). With increasing pressure, S(22°C) increases further. The correlation between S(22°C) and pressure is not linear. At a pressure level of 7.5 MPa, S(22°C) has an unusual high standard deviation. According to literature, S is higher in ab-direction than in c-direction (for hot-pressing with 10 MPa, $S_{ab} = 1.06\ S_c$ [9,10]). Due to the particle orientation during tape casting, S(22°C) is increased in ab-direction. As PAS also leads to a further texturing (see Figure 5A), the increase of S(22°C) with pressure is attributed to enhanced texture. The Seebeck coefficients at 100°C of PAS samples are in the same range as the values measured at room temperature (Figure 6B). S_{ab}(100°C) of the dry-pressed reference is 20 µV/K lower than measured at room temperature. S_{ab} of all three samples increases with temperatures until it reaches a maximum at 800°C. The slope of the specimens sintered with 7.5 MPa (linear fit between 300°C and 700°C, slope 0.04 µV/K^2) is less steep than of the two other samples (linear fit between 300°C and 700°C, slope 0.07 µV/K^2). There is no significant difference between S_{ab} of the reference and of the PAS sample pressed with 7.5 MPa above 700°C (2-sample t-test). Above 400°C, the specimens sintered with 2.5 MPa show the highest S_{ab} values, with a maximum of S(800°C) = 164 µV/K. The literature data for hot-pressed Co349 are slightly higher in the range 170-180 µV.[9,10,16]

3.4 | Electrical conductivity

The electrical conductivity at room temperature of the dry-pressed specimens is very low[2] (Figure 5C). Tape casting increases σ(22°C) by the factor of 3. With increasing pressure, σ(22°C) increases strictly monotonically. Although, the increase in conductivity from 2.5 MPa to 5 MPa and from 5 MPa to 7.5 MPa are not significant, respectively (two-sample-t-test). The large differences between the experimental points in room temperature electrical conductivity remain almost unchanged up to 900°C (Figure 6A). The temperature has only a minor influence on σ_{ab}. Due to the low density

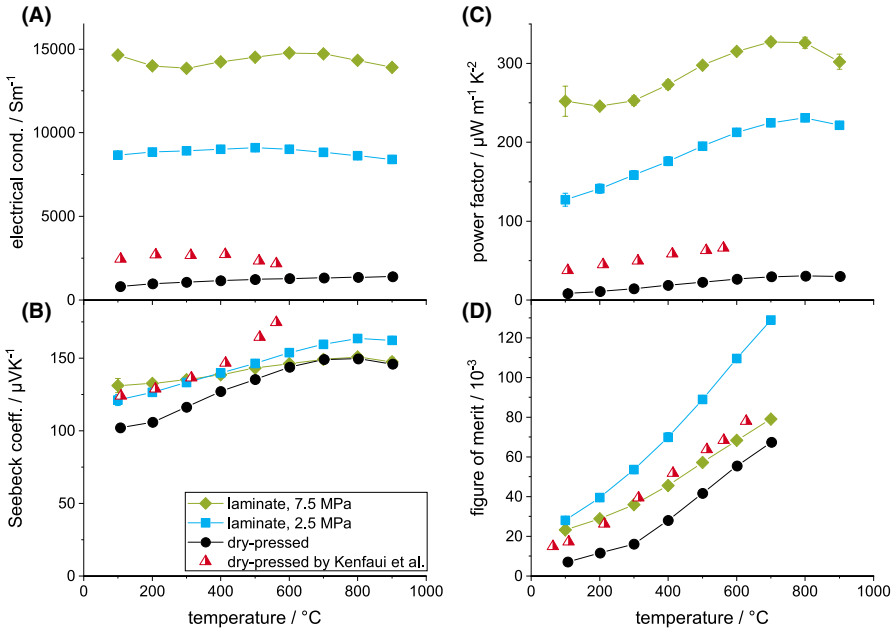

FIGURE 6 Thermoelectric properties at elevated temperatures: (A) electrical conductivity; (B) Seebeck coefficient; (C) power factor; and (D) figure of merit. Literature data (red triangles) for dry-pressed samples are derived from Kenfaui et al,[9,10] relative density amounts to 60%, thermal conductivity to 1 W/mK at room temperature. PAS samples sintered for 2h. Error bars indicate standard deviation for the Seebeck coefficient S and the electrical conductivity σ. The error bars of PF and ZT show the calculated errors according to Gaussian error propagation. To calculate ZT of PAS laminates, the thermal conductivity κ at room temperature (see Table 1) was used

of the dry-pressed sample, its electrical conductivity is lower as for similar studies.[9,14] But as shown in Figure 6A, PAS increases the electrical conductivity compared with both datasets for dry-pressed samples. The results are in the same range as for hot-pressed Co349 from other studies.[9,16] Kenfaui et al[9] reported 11 500 S/m at room temperature for hot-pressed samples with 5 MPa, Nagahama et al[18] derived 14 000 S/m at 200°C for hot-pressed samples with 8 MPa and Schulz et al[16] found 12 500 S/m at room temperature for hot-pressed samples with 10 MPa. In the latter study, the temperature dependency was much higher with an increase in 35%.

3.5 | Power factor

The dry-pressed reference has a low *PF* at room temperature. Tape casting increases the *PF*(22°C) by the factor of 3.1 due to texture. PAS with 2.5 MPa results in an increase by a factor of 10.4, and PAS with 7.5 MPa leads to a 20 times higher *PF*(22°C) with respect to the reference as both σ(22°C) and *S* are higher (Figure 5). Over temperature, *PF* increases for all three measured samples (Figure 6C). It reaches a maximum at 800°C. The results are PF_{ab}(800°C) = 30 μW/mK^2; 231 μW/mK^2, and 326 μW/mK^2 for reference, 2.5 MPa, and 7.5 MPa, respectively. This corresponds to an increase by a factor of 10.9 or 5 compared to the dry-pressed sample of this study or the one of Kenfaui et al,[9] respectively. The slopes of the PAS samples are steeper than of the dry-pressed reference. Kenfaui et al[9] and Schulz et al[16] reached slightly higher *PF*-values (T_{max} = 700°C), due to the above-explained differences in *S* and σ.

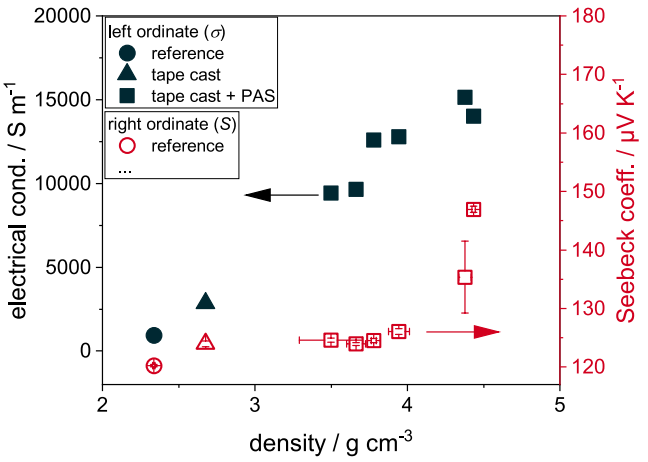

FIGURE 7 Electrical conductivity (left ordinate) and Seebeck coefficient (right ordinate) at room temperature plotted over bulk density. Error bars indicate the standard deviation

3.6 | Thermal conductivity and figure of merit

Phonon and charge carrier transport are both higher along the crystal layers of Co349.[10] Thus, the increase in σ(22°C) and density in ab-direction of the textured microstructure is accompanied by an increase in thermal conductivity κ(22°C) (see Table 1) up to a factor of 10. Measuring κ of hot-pressed samples in pressing direction (c-direction) underestimates κ as the phonon transport is interfered by the crystal layers as, for example shown in reference 16. Combining the moderate increases in κ and the strong increase in *PF*, the highest ZT_{ab}(22°C) of 0.026 is reached for PAS samples sintered under a pressure of 2.5 MPa. For all measured specimens, ZT_{ab} increases with temperature (Figure 7). Contrary to *PF* and σ, the sample sintered with 2.5 MPa shows the highest values over the full temperature range. With ZT_{ab}(700°C) = 0.13, it is almost two times higher than *ZT* of the reference. The difference between the sample sintered with 7.5 MPa and the reference is not as high as for the other properties due to the much higher thermal conductivity, κ_{ab}, of the 7.5 MPa sample. For a maximum ZT_{ab}, it is not beneficial to produce a microstructure as dense as possible. Although high densities enhance PF_{ab} largely, ZT_{ab} is reduced due to high κ in this direction. Schulz et al[16] reported very high *ZT*-values (0.29 at 600°C) for tape cast Co349 pressureless-sintered samples. As κ was measured in c-direction, the *ZT*-value is probably overestimated. The only other ZT_{ab} for hot-pressed Co349 was published by Kenfaui et al.[10] For hot-pressed samples with 10 MPa, a maximum ZT_{ab}(750°C) of 0.16 was reached. Kenfaui determined κ_{ab} for the whole temperature range. In literature,[10,16]

TABLE 2 Calculated *ZT* at 700°C *ZT*(700°C) is calculated using κ(22°C) as measured in this study. ZT_{fit}(700°C) is calculated with κ_{fit}(700°C)

	PF(700°C) in μW/mK^2	κ(22°C) in W/mK	*ZT*(700°C) with κ(22°C) in 10^{-3}	κ_{fit}(700°C) in W/mK	ZT_{fit}(700°C) with κ_{fit}(700°C) in 10^{-3}
reference	30	0.44	66	0.43	67
2.5 MPa, 2 h	225	1.70	129	**1.11**	**197**
7.5 MPa, 2 h	327	4.03	79	**2.23**	**142**

Note: All bold values were calculated using the extrapolated κ_{fit}(700°C) according to $\kappa_{fit} = A \bullet e^{(-T/B)} + C$ with A = 0.849, B = 512, C = 0.892 for 2.5 MPa derived from Shi et al[36] and A = 2.106, B = 205, C = 2.166 for 7.5 MPa.[35]

κ of hot-pressed Co349 decreases with rising measuring temperature. The κ over temperature curve is very similar for similar κ in different studies[10,16,35,36] and it can be fitted by the following equation $\kappa = A \bullet e^{(-T/B)} + C$ with absolute temperature T, and constants A, B, and C. In this study, only κ of the reference was determined over the whole temperature range. κ_{ab} was only measured at room temperature and then used to approximate ZT_{ab} for the whole temperature range. Thus, the ZT_{ab} values presented in this paper are probably underestimated. When ZT_{ab} is calculated using the extrapolated κ_{fit} based on the κ over temperature curve of similar κ from literature,[35,36] the ZT values at 700°C as shown in Table 2 are reached (ZT_{fit}). This results in ZT_{fit}(700°C) of 0.2 for 2.5MPa, which is higher than published for hot-pressed Co349 using κ_{ab}.[10,37]

3.7 | Influence of dwell time

The results in Table 1 do neither show a significant influence of the dwell time on the relative density nor on the conductivity at room temperature σ(22°C) or on PF(22°C) (two-sample t-test). Only the Seebeck coefficient S(22°C) at a pressure level of 7.5 MPa is increased significantly by an increased dwell time. It can be concluded that a prolonged dwell time during PAS is not beneficial for the thermoelectric properties.

3.8 | Effect of density and texture

The data shown in Figure 5 and Table 1 suggest a dependency of the electrical conductivity and the Seebeck coefficient at room temperature, σ(22°C) and S(22°C), respectively, on the apparent density of the specimens. Figure 7 shows the respective plots. The Seebeck coefficient increases nonlinearly with density. The reference has the lowest density and the lowest S(22°C). In the range of 2.6 g/cm^3 to 4.0 g/cm^3, S(22°C) is almost constant. The range comprises the tape cast and the PAS samples sintered with a pressure up to 5 MPa. The samples with a density above 4.3 g/cm^3 show by far the highest Seebeck coefficient. The graph leads to the assumption that the increase in S(22°C) for tape cast samples is due to the texture and not due to the increased density, as S(22°C) remains nearly constant when the density is further increased. The almost fully dense specimens have a very high Seebeck coefficient, probably due to a combined mechanism of density and texture. The Seebeck coefficient of Co349 is anisotropic.[10] A higher density of the sintered test bars leads to higher electrical conductivity, as shown in Figure 7. The correlation can be even fitted with a linear regression (R^2(adj) = 94%). But the linear correlation between electrical conductivity and density is false positive as texture and density increase simultaneously with increasing pressure during sintering. When the data presented in this paper are compared to PAS specimens with a similar density but a lower degree of texture[12] as derived by reaction sintering (see Table 3), it is obvious that a lower degree of texture (MRD = 4.1) leads to a lower electrical conductivity. Kenfaui et al[22] showed a similar effect for highly dense Co349 prepared by SPS (low MRD) and hot-pressing (high MRD). This means that the increase in electrical conductivity over pressure (see Figure 5C) is a combined mechanism of increased density and increased texture. A higher density enlarges the intergranular contact areas as porosity is decreased simultaneously. This leads to the observed higher electrical conductivity. Previous studies have shown similar dependencies for oxide thermoelectric materials.[11,31] A higher degree of texture increases the electrical conductivity in ab-direction due to the anisotropy of the material.[22]

4 | SUMMARY

This study about the influence of dwell time and pressure during pressure-assisted sintering of Co349 elucidates the following points:

1. Tape casting yields textured samples (MRD = 9.2) when conventional sintering is used. Pressure-assisted sintering (PAS) of tape-cast samples slightly increases the texture (MRD ≈ 12) and considerably increases the density.
2. A prolonged dwell time during hot-pressing is not beneficial for the thermoelectric properties. Longer dwell times do not densify the samples but coarsen the microstructure.
3. By pressure variation during sintering, the microstructure of Co349 can be tailored either toward maximum PF_{ab} as required for energy harvesting or toward maximum ZT_{ab} as required for energy recovery. This means lower

TABLE 3 Comparison between two PAS laminates with different degree of texturing, but similar density and same sintering program

	MRD	ρ in g/cm^3	ρ_{rel} in %	S in µV/K	σ in S/m	κ in W/mK
Calcined, 7.5 MPa, 2 h	12.8	4.38 ± 0.04	94 ± 1	135 ± 6	15 140 ± 1182	4.03
Reaction-sintered, 7.5 MPa, 2 h[12]	4.1	4.24 ± 0.00	91 ± 0	142 ± 2	9763 ± 1157	2.91

Note: Data for the reaction-sintered sample are derived from reference [12].

pressure for a porous microstructure and maximum ZT_{ab}, higher pressure for full densification and maximum PF_{ab}.
4. Higher applied pressures during sintering result in higher densities, in higher electrical conductivities σ_{ab}, in higher Seebeck coefficients S_{ab}, and higher power factors PF_{ab}. A pressure of 7.5 MPa increases PF_{ab}(700°C) by more than one order of magnitude to 326 $\mu W/mK^2$ compared to the dry-pressed reference from the same powder.
5. Measuring the thermal conductivity κ_{ab} for Co349 with the hot-disc method is an appropriate method to be applied for flat specimens to obtain all thermoelectric data in the same direction.
6. With increasing pressure during sintering, κ_{ab} increases. A pressure of 7.5 MPa increases κ_{ab}(22°C) by the factor of 10 compared to the reference. With respect to ZT, the high κ_{ab} nearly compensates the increase in PF for high-pressure levels.
7. The highest ZT was measured for PAS samples pressed with a moderate pressure of 2.5 MPa to ZT_{ab}(700°C) = 0.13, which is almost the double value compared to the dry-pressed reference. Lower pressures during sintering are a good compromise between texturing to enhance σ_{ab} and relative high porosity (25%) to maintain a low κ_{ab}.

ACKNOWLEDGMENTS

The authors thank their BAM colleagues F. Lindemann for the particle analysis, S. Benemann for the SEM micrographs, W. Guether for the experimental expertise, and A. Boecker for XRD analyses. They also want to thank H. Taubmann from C3 Prozess- und Analysetechnik for the hot-disc measurements. Open access funding enabled and organized by ProjektDEAL.

ORCID

Sophie Bresch https://orcid.org/0000-0003-2490-7208
Björn Mieller https://orcid.org/0000-0002-0784-9790

REFERENCES

1. Ioffe AF. Semiconductor thermoelements and thermoelectric cooling. London; 1957.
2. Fergus JW. Oxide materials for high temperature thermoelectric energy conversion. J Eur Ceram Soc. 2012;32(3):525–40.
3. Koumoto K, Funahashi R, Guilmeau E, Miyazaki Y, Weidenkaff A, Wang Y, et al. Thermoelectric ceramics for energy harvesting. J Am Ceram Soc. 2013;96(1):1–23.
4. Ryoji F, Ichiro M, Hiroshi I, Tsunehiro T, Uichiro M, Satoshi S. An oxide single crystal with high thermoelectric performance in air. Jpn J Appl Phys. 2000;39(11B):L1127.
5. Xu G, Funahashi R, Shikano M, Matsubara I, Zhou Y. Thermoelectric properties of the Bi- and Na-substituted $Ca_3Co_4O_9$ system. Appl Phys Lett. 2002;80(20):3760.
6. Liu Y, Lin Y, Jiang L, Nan C-W, Shen Z. Thermoelectric properties of Bi^{3+} substituted Co-based misfit-layered oxides. J Electroceram. 2008;21(1):748–51.
7. Su H, Jiang Y, Lan X, Liu X, Zhong H, Yu D. $Ca_{3-x}Bi_xCo_4O_9$ and $Ca_{1-y}Sm_yMnO_3$ thermoelectric materials and their power-generation devices. Phys Status Solidi. 2011;208(1):147–55.
8. Masset AC, Michel C, Maignan A, Hervieu M, Toulemonde O, Studer F, et al. Misfit-layered cobaltite with an anisotropic giant magnetoresistance: $Ca_3Co_4O_9$. Phys Rev B. 2000;62(1):166–75.
9. Kenfaui D, Chateigner D, Gomina M, Noudem JG. Anisotropy of the mechanical and thermoelectric properties of hot-pressed single-layer and multilayer thick $Ca_3Co_4O_9$ ceramics. Int J Appl Ceram Tec. 2011;8(1):214–26.
10. Kenfaui D, Lenoir B, Chateigner D, Ouladdiaf B, Gomina M, Noudem JG. Development of multilayer textured $Ca_3Co_4O_9$ materials for thermoelectric generators: Influence of the anisotropy on the transport properties. J Eur Ceram Soc. 2012;32(10):2405–14.
11. Bresch S, Mieller B, Selleng C, Stöcker T, Moos R, Rabe T. Influence of the calcination procedure on the thermoelectric properties of calcium cobaltite $Ca_3Co_4O_9$. J Electroceram. 2018;40(3):225–34.
12. Bresch S, Mieller B, Schoenauer-Kamin D, Moos R, Giovanelli F, Rabe T. Influence of pressure assisted sintering and reaction sintering on microstructure and thermoelectric properties of Bi-doped and undoped calcium cobaltite. J Appl Phys. 2019;126(7):075102.
13. Prasad R, Bhame SD. Review on texturization effects in thermoelectric oxides. Mater Renew Sustain Energy. 2020;9(1):3.
14. Boyle C, Carvillo P, Chen Y, Barbero EJ, McIntyre D, Song X. Grain boundary segregation and thermoelectric performance enhancement of bismuth doped calcium cobaltite. J Eur Ceram Soc. 2016;36(3):601–7.
15. Mistler RE, Twiname ER. Tape casting: theory and practice. Westerville, OH: American ceramic society; 2000.
16. Schulz T, Reimann T, Bochmann A, Vogel A, Capraro B, Mieller B, et al. Sintering behavior, microstructure and thermoelectric properties of calcium cobaltite thick films for transversal thermoelectric multilayer generators. J Eur Ceram Soc. 2018;38(4):1600–7.
17. Jabbari M, Bulatova R, Tok AIY, Bahl CRH, Mitsoulis E, Hattel JH. Ceramic tape casting: a review of current methods and trends with emphasis on rheological behaviour and flow analysis. Mater Sci Eng, B. 2016;212:39–61.
18. Nagahama D, Tani T, Masuda Y, Itahara H, Yonezawa T, Koumoto K. Thermoelectric Properties of $Ca_3Co_4O_9$-based Ceramics Textured by Templated Grain Growth Method. In: Proceedings of the XXI International Conference on Thermoelectrics. Long Beach, CA: IEEE; 2002. p. 211–4.
19. Torres MA, Garcia G, Urrutibeascoa I, Madre MA, Diez JC, Sotelo A. Fast preparation route to high-performances textured Sr-doped $Ca_3Co_4O_9$ thermoelectric materials through precursor powder modification. Sci China Mater. 2018;62(3):399–406.
20. Liu YH, Lin YH, Shi Z, Nan CW, Shen ZJ. Preparation of $Ca_3Co_4O_9$ and improvement of its thermoelectric properties by spark plasma sintering. J Am Ceram Soc. 2005;88(5):1337–40.
21. Delorme F, Diaz-Chao P, Giovannelli F. Effect of Ca substitution by Fe on the thermoelectric properties of $Ca_3Co_4O_9$ ceramics. J Electroceram. 2018;40(2):107–14.
22. Kenfaui D, Gomina M, Noudem J, Chateigner D. Anisotropy of transport properties correlated to grain boundary density and quantified texture in thick oriented $Ca_3Co_4O_9$ ceramics. Materials. 2018;11(7):1224.

23. Brandt B, Rabe T. Structuring of LTCC substrates by a combination of pressure-assisted sintering and hot embossing. J Ceram Sci Technal. 2015;6(4):273–8.
24. Moulson AJ, Herbert JM. Electroceramics. Chichester, England: John Wiley & Sons Ltd; 2003.
25. Jaffe B. Piezoelectric ceramics. London, England: Elsevier Science; 2012.
26. Riegel J, Neumann H, Wiedenmann HM. Exhaust gas sensors for automotive emission control. Solid State Ionics. 2002;152–153:783–800.
27. Bochmann A, Reimann T, Schulz T, Teichert S, Töpfer J. Transverse thermoelectric multilayer generator with bismuth-substituted calcium cobaltite: design optimization through variation of tilt angle. J Eur Ceram Soc. 2019;39(9):2923–9.
28. Löhnert R, Stelter M, Töpfer J. Evaluation of soft chemistry methods to synthesize Gd-doped CaMnO3−δ with improved thermoelectric properties. Mater Sci Eng, B. 2017;223(Supplement C):185–93.
29. Funahashi S, Nakamura T, Kageyama K, Ieki H. Monolithic oxide–metal composite thermoelectric generators for energy harvesting. J Appl Phys. 2011;109(12):124509.
30. Bachmann F, Hielscher R, Schaeben H. Texture analysis with MTEX – free and open source software toolbox. Solid State Phenom. 2010;160:63–8.
31. Bresch S, Mieller B, Delorme F, Chen C, Bektas M, Moos R, et al. Influence of reaction-sintering and calcination conditions on thermoelectric properties of Sm-doped calcium manganate $CaMnO_3$. J Ceram Sci Technol. 2018;9(3):289–99.
32. Stöcker T, Exner J, Schubert M, Streibl M, Moos R. Influence of oxygen partial pressure during processing on the thermoelectric properties of aerosol-deposited $CuFeO_2$. Materials. 2016;9(4):227.
33. German RM. Sintering theory and practice. Hoboken, New Jersey, US: John Wiley & Sons; 1996.
34. Sotelo A, Costa FM, Ferreira NM, Kovalevsky A, Ferro MC, Amaral VS, et al. Tailoring $Ca_3Co_4O_9$ microstructure and performances using a transient liquid phase sintering additive. J Eur Ceram Soc. 2016;36(4):1025–32.
35. Schulz T, Töpfer J. Thermoelectric properties of $Ca_3Co_4O_9$ ceramics prepared by an alternative pressure-less sintering/annealing method. J Alloys Compd. 2016;659:122–6.
36. Shi Z, Xu J, Zhu J, Zhang Y, Gao T, Qin M, et al. Effect of platelet template seeds on microstructure and thermoelectric properties of $Ca_3Co_4O_9$ ceramics. Ceram Int. 2019;45(2):1977–83.
37. Itahara H, Tani T. Highly-textured thermoelectric oxide polycrystals synthesized by the reactive-templated grain growth (RTGG) method. Toyota R&D Review of Toyota CRDL. 2004;39(1):63–70.

How to cite this article: Bresch S, Mieller B, Schönauer-Kamin D, et al. Influence of pressure and dwell time on pressure-assisted sintering of calcium cobaltite. *J Am Ceram Soc*. 2020;00:1–11. https://doi.org/10.1111/jace.17541